

VLBA DETERMINATION OF THE DISTANCE TO NEARBY STAR-FORMING REGIONS. VIII.  
THE LKH $\alpha$  101 CLUSTER

SERGIO A. DZIB,<sup>1</sup> GISELA N. ORTIZ-LEÓN,<sup>1,2</sup> L. LOINARD,<sup>3,4</sup> A. J. MIODUSZEWSKI,<sup>5</sup> L. F. RODRÍGUEZ,<sup>3</sup> S.-N. X. MEDINA,<sup>1</sup> AND  
R. M. TORRES<sup>6</sup>

<sup>1</sup>*Max-Planck-Institut für Radioastronomie, Auf dem Hügel 69, D-53121 Bonn, Germany*

<sup>2</sup>*Humboldt Fellow*

<sup>3</sup>*Instituto de Radioastronomía y Astrofísica, Universidad Nacional Autónoma de México, Morelia 58089, Mexico*

<sup>4</sup>*Instituto de Astronomía, Universidad Nacional Autónoma de México, Apartado Postal 70-264, CdMx C.P. 04510, Mexico*

<sup>5</sup>*National Radio Astronomy Observatory, P.O. Box 0, Socorro, NM 87801, USA*

<sup>6</sup>*Centro Universitario de Tonalá, Universidad de Guadalajara, Avenida Nuevo Periférico No. 555, Ejido Dan José Tatepozco, C.P. 48525, Tonalá, Jalisco, México.*

ABSTRACT

The LkH $\alpha$  101 cluster takes its name from its more massive member, the LkH $\alpha$  101 star, which is an  $\sim 15 M_{\odot}$  star whose true nature is still unknown. The distance to the LkH $\alpha$  101 cluster has been controversial for the last few decades, with estimated values ranging from 160 to 800 pc. We have observed members and candidate members of the LkH $\alpha$  101 cluster with signs of magnetic activity, using the Very Long Baseline Array, in order to measure their trigonometric parallax and, thus, obtain a direct measurement of their distances. A young star member, LkH $\alpha$  101 VLA J043001.15+351724.6, was detected at four epochs as a single radio source. The best fit to its displacement on the plane of the sky yields a distance of  $535 \pm 29$  pc. We argue that this is the distance to the LkH $\alpha$  101 cluster.

*Keywords:* astrometry — stars:formation — stars: individual (LKH $\alpha$  101) — techniques: interferometric

arXiv:1801.05231v1 [astro-ph.SR] 16 Jan 2018

## 1. INTRODUCTION

LkH $\alpha$  101 is a massive star,  $M \sim 15 M_{\odot}$ , with an extinction of  $A_V \simeq 10$ . It illuminates the reflection nebula NGC 1579 and has a directly imaged disk (see the review by [Andrews & Wolk 2008](#), and references therein). It also hosts a small HII region that is sustained by the ionized winds from its disk ([Thum et al. 2013](#)). LkH $\alpha$  101 is associated with a cluster of young low-mass stars (hereafter, the LkH $\alpha$  101 cluster), some of which are magnetically active ([Becker & White 1988](#); [Stine & O’Neal 1998](#); [Osten & Wolk 2009](#)). These properties strongly suggest that LkH $\alpha$  101 is a young high-mass star. However, there is an absence of stellar absorption features and, thus, there is no classification for its photosphere ([Herbig et al. 2004](#)). In fact, its spectroscopic properties have been compared to some post-main-sequence massive stars. As has been discussed by [Andrews & Wolk \(2008\)](#), the true nature of LkH $\alpha$  101 is still a mystery and this problem is compounded by its large distance uncertainty.

An extended discussion of the different suggested distances to the LkH $\alpha$  101 cluster (which includes the LkH $\alpha$  101 star) has been presented in the review by [Andrews & Wolk \(2008\)](#) and we summarize it here. Initially, [Herbig \(1971\)](#) estimated a distance of 800 pc based on UVB photometry of two nearby early B-type stars. Later, [Stine & O’Neal \(1998\)](#) suggested an entirely different value of 160 pc, arguing that the radio luminosities of T Tauri stars in the LkH $\alpha$  101 cluster would be incompatible with that of T Tauri stars in Taurus-Aurigae if the cluster were at 800 pc. However, [Herbig et al. \(2004\)](#) noted that this method is inadvisable. [Tuthill et al. \(2002\)](#) favored a value of  $d \simeq 340$  pc, from model constraints on the star-disk mass for LkH $\alpha$  101 and the proper motions of a companion. [Herbig et al. \(2004\)](#) obtained spectral parallax measurements to 40 young LkH $\alpha$  101 cluster members with a wide range of spectral types and estimated  $d \simeq 700 \pm 200$  pc. The conclusion of the discussion by [Andrews & Wolk \(2008\)](#) was that most of the observational constraints suggest a distance between 500 pc to 700 pc. These authors also noted that the two different methods to identify cluster membership, by [Feigelson & Montmerle \(1999\)](#) and [Feigelson et al. \(2005\)](#), are in good agreement when applied to the LkH $\alpha$  101 cluster if its distance is about 550 pc. Clearly, the past suggested distances to the cluster have very large uncertainties because they are based only on interpretations of the properties of the stars. To date, there are no direct measurements of distances to any of the members of the LkH $\alpha$  101 cluster and the most common assumed distance is 700 pc. An accurate distance to this region is fundamental to constrain the true nature of the LkH $\alpha$  101 star.

Magnetically active young stars are excellent targets to measure trigonometric parallax and, thus, determine direct distances. They can be observed with the Very Long Baseline Interferometry (VLBI) technique (see [Dzib et al. 2016](#);

[Ortiz-León et al. 2017a,b](#); [Kounkel et al. 2017](#), for recent results). By employing this technique, we observed suspected magnetically active young stars in the LkH $\alpha$  101 cluster to measure their distance and provide a more accurate distance to the cluster.

## 2. OBSERVATIONS AND DATA CALIBRATION

We observed six young star members and a candidate member of the LkH $\alpha$  101 cluster. These target sources are listed in Table 1. We used the Very Long Baseline Array (VLBA; [Napier et al. 1994](#)), operated by the Long Baseline Observatory (LBO), under projects BD165 and BD207. The observations used the multi-phase center capability provided by the VLBA DifX digital correlator ([Deller et al. 2011](#)). The observations of the first project were carried out on 2012 October 9 and October 11, at a wavelength of 3.6 cm ( $\nu = 8.42$  GHz). In the first session (October 9), the first four targets in Table 1 were observed, while the other three were observed as part of the second session (October 11). Following the successful detections of three target sources, we initiated a series of multi-epoch observations (project BD207) at a wavelength of 6.0 cm ( $\nu = 4.5$  GHz) starting in 2017 March and, subsequently, we obtained a new observation every three months. The change of receiver was due to three reasons. First, the primary beam size is larger and we can cover all seven sources in a single pointing. Second, the new 6.0 cm band receiver is more sensitive than the 3.6 cm receiver. Finally, because of their negative spectral indices, the target sources are brighter at longer wavelengths. These last two reasons increase the SNR of the detection, increasing the precision of the position measurement.

**Table 1.** Observed sources. The names and infrared classes from [Osten & Wolk \(2009\)](#).

Name (LkH $\alpha$ 101 VLA)	IR	
	Class	Detected?
J043010.87+351922.4	III	No
J043016.04+351726.9	III	No
J043017.90+351510.0 <sup>a</sup>	...	Yes
J043019.14+351745.6	II	Yes
J042953.98+351848.2	III	No
J043001.15+351724.6 <sup>b</sup>	III	Yes
J043002.64+351514.9	II	No

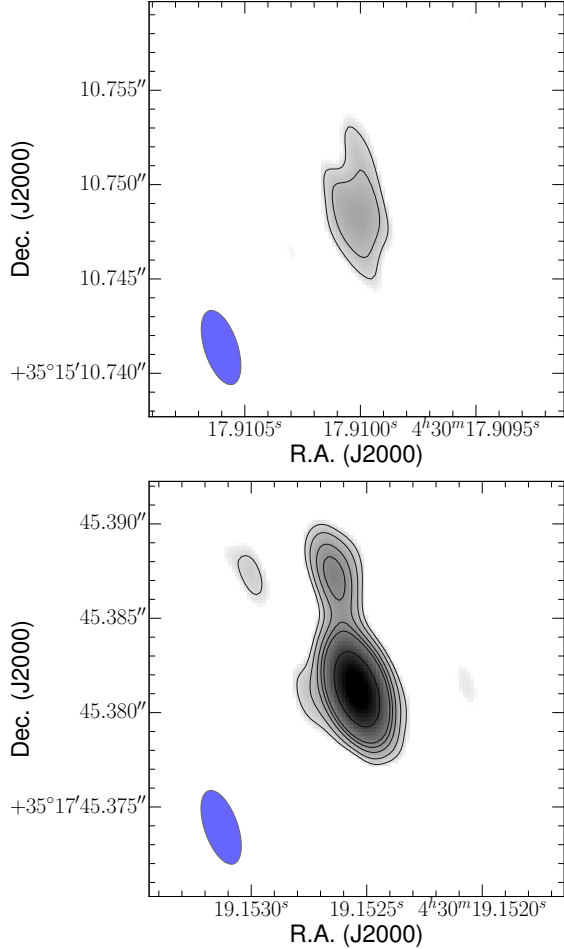
<sup>a</sup>Candidate member.

<sup>b</sup>This paper is based on the detections of this star.

The observations of the targets were recorded as part of cycles with two minutes spent on-source and one minute spent on the main phase calibrator, J0429+3319. To improve the

**Table 2.** Observation dates, synthesized beam size, and noise levels of the final maps around LkH $\alpha$  101 VLA J043001.15+351724.6, as well as measured source position and flux densities.

Mean UT date (yyyy.mm.dd/hh:mm)	Julian Day	Synthesized beam ( $\theta_{\text{maj}} \times \theta_{\text{min}}$ ; P.A.)	$\sigma_{\text{noise}}$ ( $\mu\text{Jy beam}^{-1}$ )	$\alpha$ (J2000.0) 04 <sup>h</sup> 30 <sup>m</sup>	$\sigma_{\alpha}$	$\delta$ (J2000.0) 35° 17'	$\sigma_{\delta}$	$f_{\nu}$ (mJy)
2012.10.09/10:17	2456211.93	0''0021 $\times$ 0''0008; 6.5°	36	1 <sup>s</sup> .146281	0 <sup>s</sup> .000006	24 <sup>m</sup> .43957	0 <sup>m</sup> .00014	0.26 $\pm$ 0.04
2017.03.25/21:46	2457838.41	0''0036 $\times$ 0''0012; 18.6°	23	1 <sup>s</sup> .146702	0 <sup>s</sup> .000008	24 <sup>m</sup> .41308	0 <sup>m</sup> .00017	0.20 $\pm$ 0.02
2017.06.17/16:16	2457922.18	0''0034 $\times$ 0''0012; 15.4°	21	1 <sup>s</sup> .146934	0 <sup>s</sup> .000007	24 <sup>m</sup> .41223	0 <sup>m</sup> .00022	0.16 $\pm$ 0.02
2017.09.11/10:38	2458007.94	0''0046 $\times$ 0''0015; -1.0°	27	1 <sup>s</sup> .147056	0 <sup>s</sup> .000002	24 <sup>m</sup> .41143	0 <sup>m</sup> .00007	0.81 $\pm$ 0.05

**Figure 1.** LkH $\alpha$  101 VLA J043017.90+351510.0 (top) and LkH $\alpha$  101 VLA J043019.14+351745.6 (bottom) as detected on 2017 March 25. The noise levels are 31  $\mu\text{Jy beam}^{-1}$  and 38  $\mu\text{Jy beam}^{-1}$  for the top and bottom images, respectively. The contour levels are -3, 4, 6, 9, 12, 15, 30, and 50 times the noise level. The size of the synthesized primary beam for both images is 4.1 mas  $\times$  1.6 mas; P.A.= 18.°5, and is displayed as a filled blue ellipse in the bottom left corner of each image.

quality of the phase calibration, we also observed every 30 minutes the secondary calibrators J0443+3441, J0414+3418, and J0418+3801. Additionally, about two dozen ICRF

quasars distributed over the entire visible sky were observed during the observations (conforming the so-called *geodetic blocks*); those are used to improve tropospheric calibration (e.g., Reid & Brunthaler 2004). These geodetic blocks were observed at the beginning and at the end of each epoch. The observation lengths of each epoch were 3.0 and 2.5 hours for the projects BD165 and BD207, respectively.

The data were edited and calibrated using the Astronomical Image Processing System (AIPS; Greisen 2003). The basic data reduction followed the standard VLBA procedure for phase-referenced observations, including the multi-calibrator schemes<sup>1</sup> and the tropospheric and clock corrections obtained from the geodetic blocks (see Loinard et al. 2007; Torres et al. 2007; Dzib et al. 2010, for a detailed description of these calibration steps). After calibration, the visibilities were first imaged with a pixel size of 100  $\mu\text{as}$  using a natural weighting scheme (ROBUST = 5 in AIPS) and covering an area of  $\sim 1$  square arcsecond. As this scheme provides the best possible noise level, we used these images to search for source detections. When a detection was obtained, we constructed new images, around the source, with a weighting scheme intermediate between natural and uniform (ROBUST = 0) using a pixel size of 50  $\mu\text{as}$ . In these last images we lost some sensitivity, but gained some angular resolution, enabling a slightly better determination of the source positions at each epoch. These images were then also corrected for the response of the primary beam. The r.m.s. noise levels,  $\sigma_{\text{noise}}$ , in the final images were 21 – 36  $\mu\text{Jy beam}^{-1}$ . The parameters of the images obtained at individual epochs are given in Table 2. From these images, the source position, flux, and deconvolved size were determined by using a two-dimensional fitting procedure (task JMFIT in AIPS).

### 3. RESULTS

Three of the target sources were detected in our observations (see Figures 1 and 2, and Table 1). LkH $\alpha$  101 VLA 043001.15+351724.6 and LkH $\alpha$  101 VLA 043017.90+351510.0

<sup>1</sup> The phase transfer from the main calibrator to the secondary calibrator J0414+3418 did not work properly, so the latter source was excluded from the multi-calibrator correction.

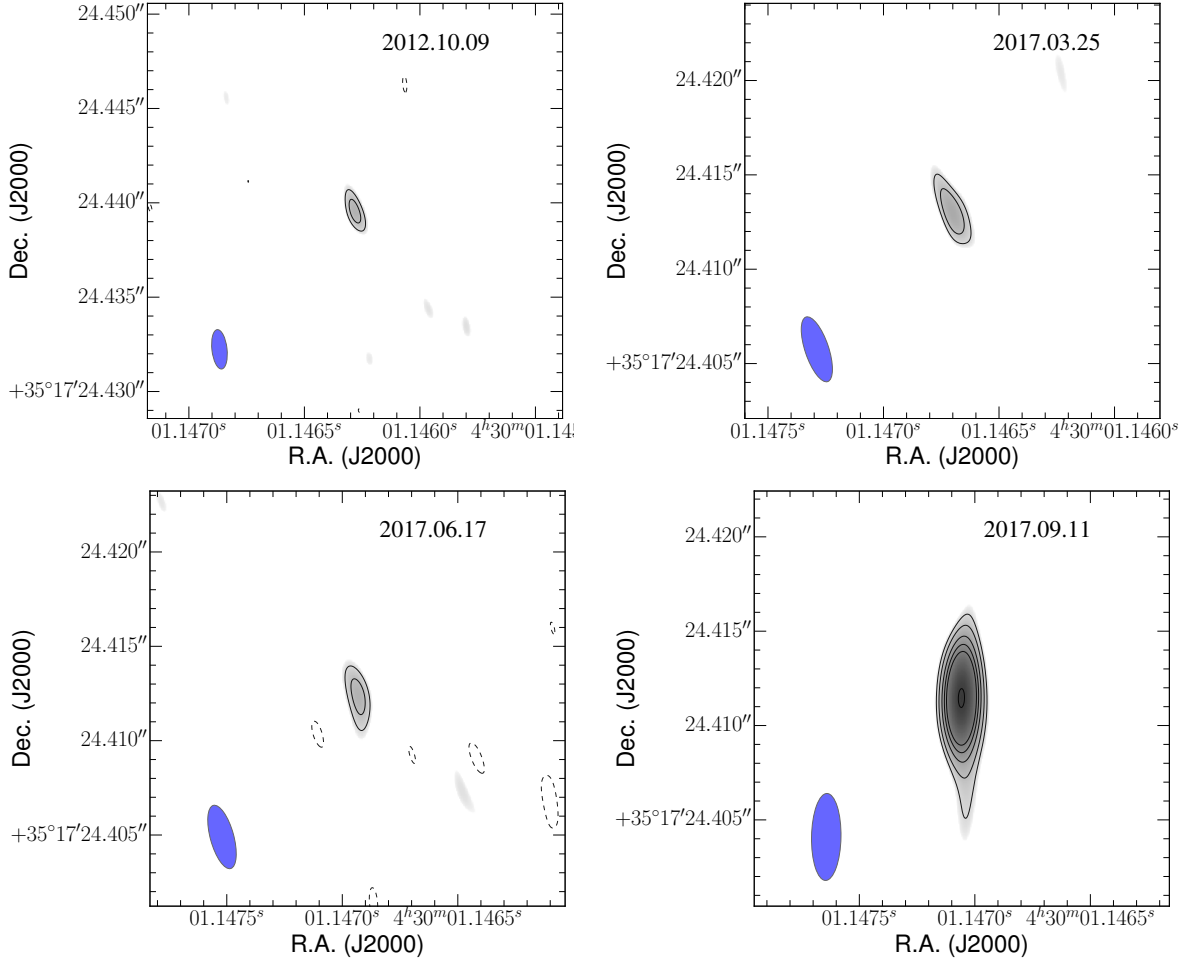


**Figure 2.** LkH $\alpha$  101 VLA J043001.15+351724.6 as detected in each epoch. The contour levels are as in Figure 1. The noise levels and the size of the synthesized primary beams are listed in Table 2. The latter are displayed as filled blue ellipses in the bottom left corner of each image.

were detected as single compact radio sources in all four epochs. LkH $\alpha$  101 VLA 043019.15+351745.6, on the contrary, had a more complex morphology. In the first epoch a single source was detected, however in the last three epochs we detected two sources in each image (e.g., bottom of Figure 1). This multi-epoch detection of two radio sources indicates that LkH $\alpha$  101 VLA J043019.14+351745.6 is a possible tight binary system, and it will be interesting for further study.

The position of the source related to LkH $\alpha$  101 VLA 043017.90+351510.0 did not significantly change between the different epochs suggesting that it is a background object and not a member of the LkH $\alpha$  101 cluster. The complexity of LkH $\alpha$  101 VLA J043019.14+351745.6 and the low number of detections make it difficult to perform an accurate astrometric analysis. This system will be further analyzed in a future paper when more observations are collected. The young star LkH $\alpha$  101 VLA 043001.15+351724.4 was well detected in four epochs and we will focus our astrometric analysis on it. In the three first detected epochs, JMFIT can-

not deconvolve LkH $\alpha$  101 VLA J043001.15+351724.6 to a finite size. The fourth epoch is also consistent with a point source, although it would also be consistent with a deconvolved size up to  $0''.0022 \times 0''.0004$ ; P.A.= $33^\circ$ . Thus the target at this epoch might be marginally resolved (on account of the unresolved nature of the source at the other epochs, we consider that it is more likely that the data contain remaining phase errors). The images of its radio emission at all epochs are shown in Figure 2.

### 3.1. Astrometry

The displacement of LkH $\alpha$  101 VLA 043001.15+351724.4 on the plane of the sky can be modeled as a combination of a trigonometric parallax ( $\varpi$ ) and linear proper motions ( $\mu$ ) (e.g. Loïnard et al. 2007). The fluxes and measured equatorial positions are presented in Table 2. The barycentric coordinates of the Earth appropriate for each observation were calculated using the NOVAS routines distributed by the US Naval Observatory. The reference epoch was taken at JD 2457108.94  $\equiv$  J2015.24, the mean epoch of the observations. The best

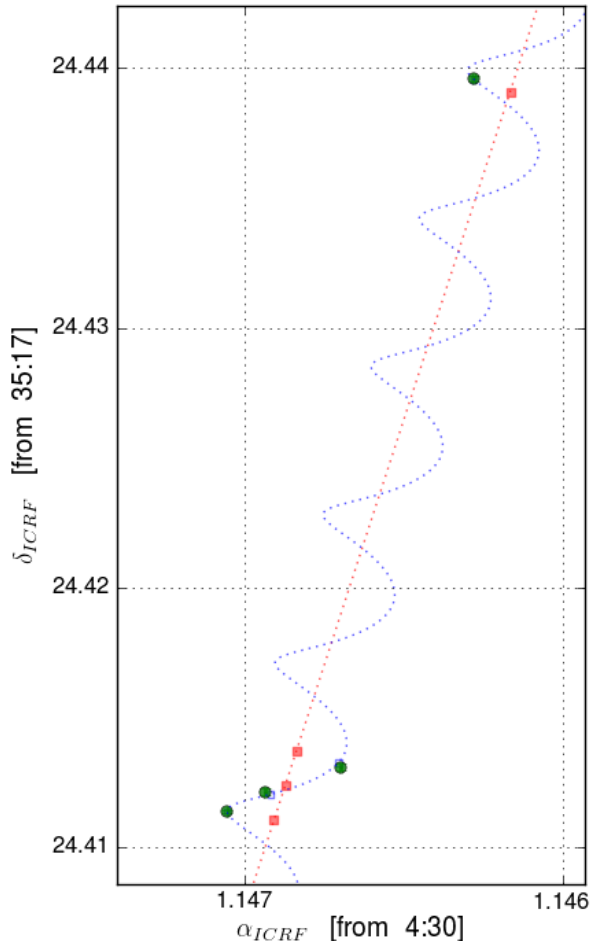


**Figure 3.** Measured positions (green circles) and best fit to the movement (dotted blue line) of LkH $\alpha$  101 VLA J043001.15+351724.6. Blue squares indicate the expected position from the best fit model. The red dotted line is the model after subtracting the reflex movement of the trigonometric parallax. The red squares indicate the position of the source at the observed epochs expected from the model after correction for reflex parallax motion.

fit to the data assuming a uniform proper motion (Figure 3) yields the following astrometric elements:

$$\alpha_{J2015.24} = 04^{\text{h}}30^{\text{m}}01^{\text{s}}.146538 \pm 0^{\text{s}}.000009$$

$$\delta_{J2015.24} = 35^{\circ}17'24''.4251 \pm 0''.0001$$

$$\mu_{\alpha} \cos \delta = 1.86 \pm 0.04 \text{ mas yr}^{-1}$$

$$\mu_{\delta} = -5.70 \pm 0.05 \text{ mas yr}^{-1}$$

$$\varpi = 1.87 \pm 0.10 \text{ mas.}$$

This parallax corresponds to a distance of  $d = 535 \pm 29$  pc. The post-fit r.m.s. values are 0.15 and 0.16 mas in right ascension and declination, respectively. Systematic errors of 0.10 and 0.13 mas (in right ascension and declination, respectively), were added in quadrature to the uncertainties delivered by JMFIT to obtain a reduced  $\chi^2 = 1$ .

#### 4. DISCUSSION AND CONCLUSION

The measurement of a trigonometric parallax is independent of any assumption of the properties of the star, since it is a purely geometric method. Consequently, this is a direct determination of distances.

The young star LkH $\alpha$  101 VLA J043001.15+351724.6 is a *bona fide* member of the LkH $\alpha$  101 cluster (Herbig et al. 2004; Osten & Wolk 2009). Therefore, its distance gives us an accurate approach on the distance to this cluster. The angular size of the cluster is  $\sim 8'$ , corresponding to a physical size of 1.25 pc at the distance of 535 pc. Because this size is much smaller than our distance error we can safely assume that the distance to the cluster, including the LkH $\alpha$  101 star, its most massive member, is also  $535 \pm 29$  pc. This result confirms the suggestion by Andrews & Wolk (2008) that the distance to the LkH $\alpha$  101 cluster ranges between 500 to 700 pc, and whom also favored a distance of 550 pc. Given this range of values, our result has reduced the uncertainty on the distance to the LkH $\alpha$  101 cluster by a factor of three. Considering that this is the first direct measurement of a distance to one of the star members of the LkH $\alpha$  101 cluster, our result is also the most well founded distance to the cluster until now.

G.-N.O.L acknowledges support from the Alexander von Humboldt Foundation in the form of a Humboldt Fellowship. L.L. and L.R. acknowledges the financial support of DGAPA, UNAM (project IN112417), and CONACyT, México. S.-N.X.M. acknowledges IMPRS for a Ph.D. research scholarship. The Long Baseline Observatory is a facility of the National Science Foundation operated under cooperative agreement by Associated Universities, Inc.

*Software:* AIPS (Greisen 2003).

#### REFERENCES

- Andrews, S. M. & Wolk, S. J. 2008, The LkH $\alpha$  101 Cluster, ed. B. Reipurth, 390
- Becker, R. H. & White, R. L. 1988, ApJ, 324, 893

- Deller, A. T., Brisken, W. F., Phillips, C. J., et al. 2011, *PASP*, 123, 275
- Dzib, S., Loinard, L., Mioduszewski, A. J., et al. 2010, *ApJ*, 718, 610
- Dzib, S. A., Ortiz-León, G. N., Loinard, L., et al. 2016, *ApJ*, 826, 201
- Feigelson, E. D., Getman, K., Townsley, L., et al. 2005, *ApJS*, 160, 379
- Feigelson, E. D. & Montmerle, T. 1999, *ARA&A*, 37, 363
- Greisen, E. W. 2003, *Information Handling in Astronomy - Historical Vistas*, 285, 109
- Herbig, G. H. 1971, *ApJ*, 169, 537
- Herbig, G. H., Andrews, S. M., & Dahm, S. E. 2004, *AJ*, 128, 1233
- Kounkel, M., Hartmann, L., Loinard, L., et al. 2017, *ApJ*, 834, 142
- Loinard, L., Torres, R. M., Mioduszewski, A. J., et al. 2007, *ApJ*, 671, 546
- Napier, P. J., Bagri, D. S., Clark, B. G., et al. 1994, *IEEE Proceedings*, 82, 658
- Ortiz-León, G. N., Dzib, S. A., Kounkel, M. A., et al. 2017a, *ApJ*, 834, 143
- Ortiz-León, G. N., Loinard, L., Kounkel, M. A., et al. 2017b, *ApJ*, 834, 141
- Osten, R. A. & Wolk, S. J. 2009, *ApJ*, 691, 1128
- Reid, M. J. & Brunthaler, A. 2004, *ApJ*, 616, 872
- Stine, P. C. & O'Neal, D. 1998, *AJ*, 116, 890
- Thum, C., Neri, R., Báez-Rubio, A., & Krips, M. 2013, *A&A*, 556, A129
- Torres, R. M., Loinard, L., Mioduszewski, A. J., & Rodríguez, L. F. 2007, *ApJ*, 671, 1813
- Tuthill, P. G., Monnier, J. D., Danchi, W. C., Hale, D. D. S., & Townes, C. H. 2002, *ApJ*, 577, 826